Supporting Information for

Exploration of oxyfluoride frameworks as Na-ion cathodes

Debolina Deb and Gopalakrishnan Sai Gautam*

Department of Materials Engineering, Indian Institute of Science, Bengaluru 560012, India

E-mail: saigautamg@iisc.ac.in

Projector Augmented Wave potentials

Table S1: Projector augmented wave potentials used to describe the core electrons of each atomic species.

ELEMENT	POTENTIAL
Na	Na_pv 19Sep2006
Ti	Ti_pv 07Sep2000
V	V_pv 07Sep2000
Cr	Cr_pv 02Aug2007
Mn	Mn_pv 02Aug2007
Fe	Fe_pv 02Aug2007
Co	Co_pv 23Apr2009
Ni	Ni_pv 06Sep2000
O	O 08Apr2002
F	F 08Apr2002

Choice of Hubbard U

Table S2: Comparison between experimental and the Hubbard U corrected strongly constrained and appropriately normed (SCAN+U) computed voltages. U values used were derived from experimental enthalpy data of transition metal oxides (TMOs) and transition metal fluorides (TMFs) for Ti (in $TiOF_2 \rightarrow Li_{0.5}TiOF_2$[1]) and V (in $VO_2F \rightarrow LiVO_2F$[2]). The U values based on TMOs and TMFs were derived in previous studies.[3,4] For Li_xTiOF_2 system, the experimental study reports a voltage range for intercalation rather than an average value.

$TiOF_2 \leftrightarrow Li_{0.5}TiOF_2$		$VO_2F \leftrightarrow LiVO_2F$	
METHOD	**VOLTAGE (V)**	**METHOD**	**VOLTAGE (V)**
Experimental	2.8 - 1	Experimental	2.9815
U in TMO (2.5 eV)	2.80252	U in TMO (1 eV)	3.3022
U in TMF (4.5 eV)	3.27898	U in TMF (4.2 eV)	4.2013

Determination of additional Na sites

Several O-rich 3*d* transition metal oxyfluorides (TMOFs), i.e., $NaMO_2F$ with M= Ti, V, Mn, Fe, and Co, are predicted to crystallize in the monoclinic (*P2/b*) space-group. However, due to absence of any monoclinic A_2MO_3 perovskite in the inorganic crystal structure database (ICSD),[5] where A could be any cation, the site coordinates for the accommodation of an additional Na-ion in monoclinic $NaMO_2F$ must be determined theoretically, with the constraint of minimizing electrostatic repulsion between the existing and introduced Na. **Figure S1** illustrates the calculation of the coordinates for the additional Na sites, as well as the displaced positions of the existing Na sites. The calculation for the site labelled 'Na3' has been used as a reference in $NaTiO_2F$ (see top half of **Figure S1**), where Na3 is displaced to its new position with coordinates (A3, B3, C3), while the additional Na will occupy the (a3, b3, c3) site. The same calculation process is followed for all Na-ions present in monoclinic $NaMO_2F$.

For $NaNiO_2F$, the lowest energy polymorph is an orthorhombic lattice, and its lattice parameters are similar to the monoclinic-$NaMO_2F$. Thus, we used a calculation procedure similar to the monoclinic polymorph for the orthorhombic as well, indicated by the reference calculation for the 'Na3' site showed in the bottom half of **Figure S1**. In the case of $NaCrO_2F$, the ground state polymorph is rhombohedral ($R\overline{3}c$). We used the additional Li sites from rhombohedral Li_2ReO_3 from the ICSD (Collection ID: 200999) as the additional Na sites in $NaCrO_2F$.

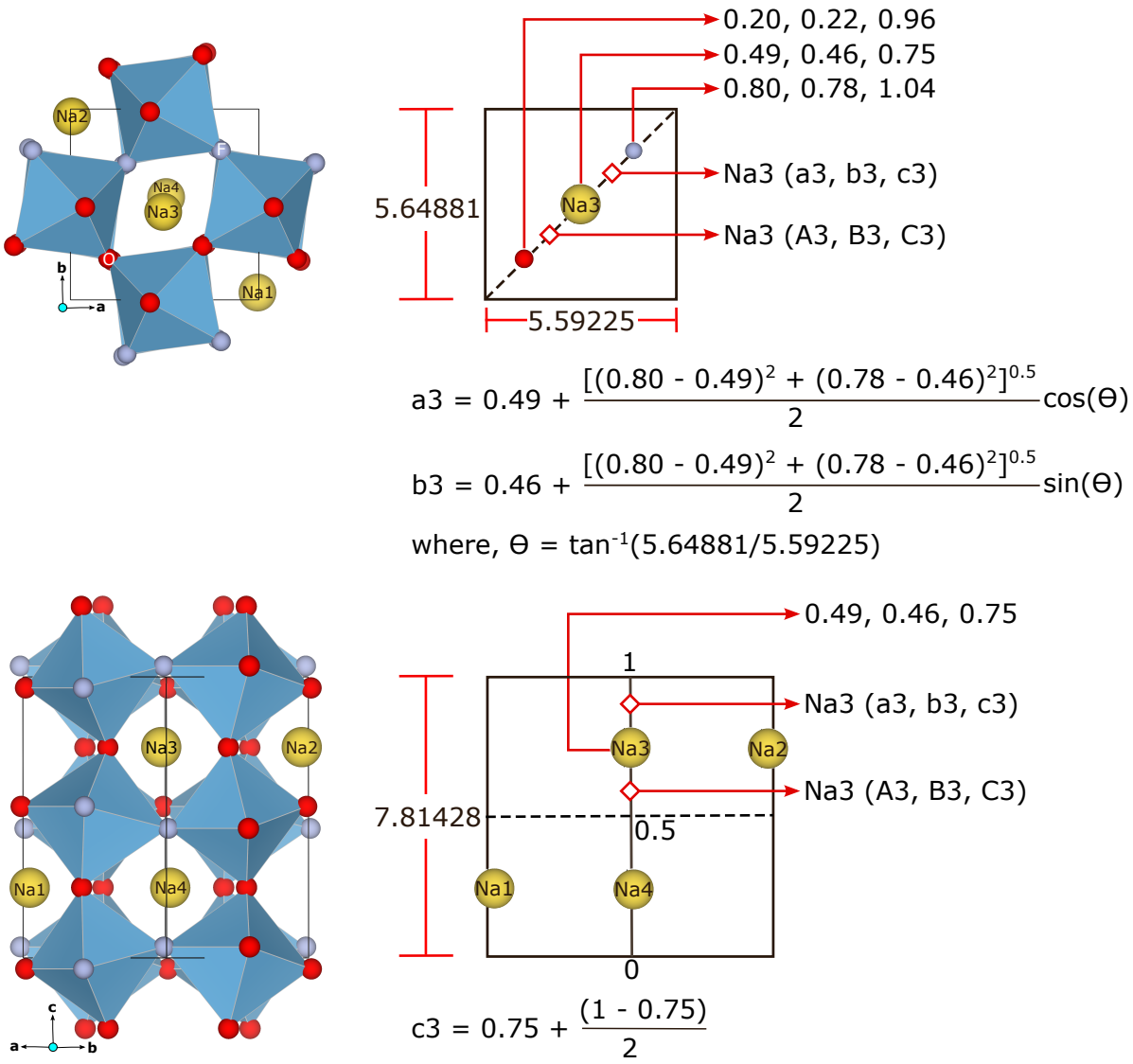

Figure S1: Determination of the additional Na site coordinates in monoclinic $NaTiO_2F$ (top half) and $NaNiO_2F$ (bottom half) is demonstrated. The calculation for the 'Na3' site is used as a reference. The existing Na3 site shifts to the (A3, B3, C3) coordinates, while the new Na site is added at (a3, b3, c3) coordinates. In monoclinic $NaTiO_2F$ the new Na sites are introduced along the face-diagonal, while in orthorhombic-$NaNiO_2F$ the sites are introduced along the *c*-axis. The blue polyhedra represent TiO_4F_2/NiO_4F_2 octahedra, and the yellow spheres are Na sites/atoms. Red and grey spheres are O and F atoms, respectively. The solid black line denotes the unit cell.

Identification of groundstate polymorph

Table S3: Percentage normalised relative energies between the groundstate and higher energy polymorphs of charged perovskites, namely O-rich $NaMOF_2$ and F-rich MOF_2 (M= 3*d* transition metal). Ground states and highest energy polymorphs are represented by 0% (blue fonts) and 100% (red fonts), respectively.

O-rich $NaMO_2F$

$NaMO_2F$	$Pm\bar{3}m$	$P4mm$	$Pbnm$	$P63/mmc$	$R\bar{3}c$	$P2/b$
$NaTiO_2F$	87.57	100.00	3.90	73.46	9.90	0.00
$NaVO_2F$	40.97	100.00	2.98	47.14	14.49	0.00
$NaCrO_2F$	57.61	100.00	0.00	8.67	9.15	9.97
$NaMnO_2F$	83.12	100.00	7.58	7.23	20.25	0.00
$NaFeO_2F$	47.94	90.83	2.44	100.00	1.05	0.00
$NaCoO_2F$	52.57	100.00	4.84	50.19	4.42	0.00
$NaNiO_2F$	40.63	100.00	2.39	84.52	0.00	0.20

F-rich MOF_2

MOF_2	$Pm\bar{3}m$	$P4mm$	$Pbnm$	$P63/mmc$	$R\bar{3}c$	$P2/b$
$TiOF_2$	39.64	93.62	0.00	100.00	0.37	0.04
VOF_2	30.17	35.10	0.00	100.00	2.19	1.15
$CrOF_2$	46.58	51.93	5.04	100.00	0.00	2.44
$MnOF_2$	15.54	100.00	6.74	45.11	0.00	5.18
$FeOF_2$	59.67	50.14	0.00	100.00	49.99	43.97
$CoOF_2$	47.86	66.81	40.90	100.00	43.47	0.00
$NiOF_2$	36.31	100.00	8.88	51.84	0.00	8.56

Table S4: Relative energies between the groundstate and higher energy polymorphs of charged perovskites, namely O-rich $NaMOF_2$ and F-rich MOF_2 (M= $3d$ transition metal). Ground states and highest energy polymorphs are represented by blue fonts and red fonts, respectively. All energies are in units of eV/f.u.

O-rich $NaMO_2F$

$NaMO_2F$	$Pm\bar{3}m$	$P4mm$	$Pbnm$	$P63/mmc$	$R\bar{3}c$	$P2/b$
$NaTiO_2F$	0.343	0.392	0.015	0.288	0.039	0.000
$NaVO_2F$	0.132	0.323	0.010	0.152	0.047	0.000
$NaCrO_2F$	0.311	0.541	0.000	0.047	0.049	0.054
$NaMnO_2F$	0.378	0.455	0.034	0.033	0.092	0.000
$NaFeO_2F$	0.067	0.127	0.003	0.139	0.001	0.000
$NaCoO_2F$	0.109	0.208	0.010	0.104	0.009	0.000
$NaNiO_2F$	0.505	1.242	0.030	1.050	0.000	0.002

F-rich MOF_2

MOF_2	$Pm\bar{3}m$	$P4mm$	$Pbnm$	$P63/mmc$	$R\bar{3}c$	$P2/b$
$TiOF_2$	0.128	0.303	0.000	0.323	0.001	0.000135
VOF_2	0.095	0.110	0.000	0.315	0.007	0.004
$CrOF_2$	0.175	0.195	0.019	0.376	0.000	0.009
$MnOF_2$	0.078	0.501	0.034	0.226	0.000	0.026
$FeOF_2$	0.387	0.326	0.000	0.649	0.325	0.285
$CoOF_2$	0.264	0.369	0.226	0.552	0.240	0.000
$NiOF_2$	0.156	0.429	0.038	0.222	0.000	0.037

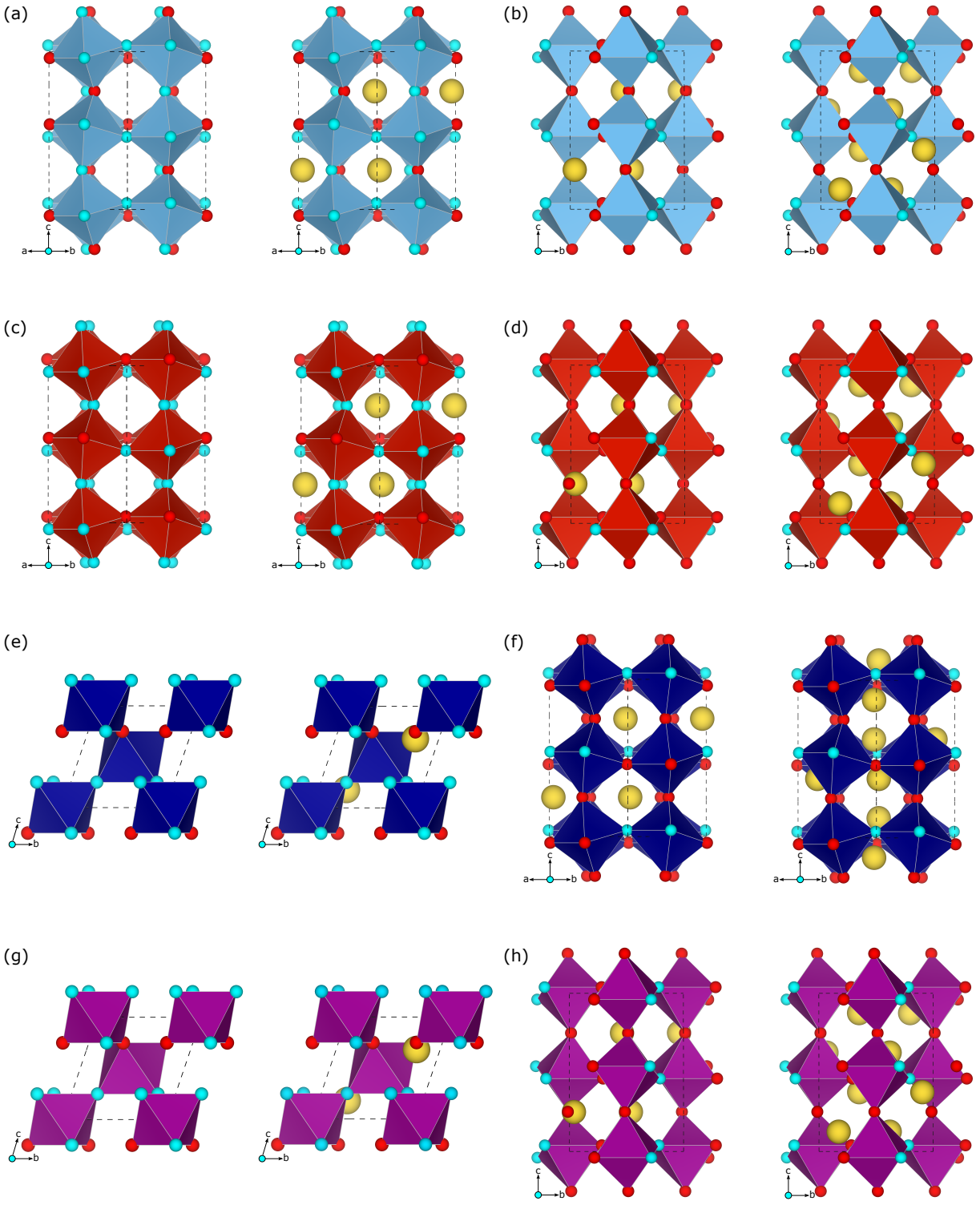
(a)
(b)
(c)
(d)
(e)
(f)
(g)
(h)

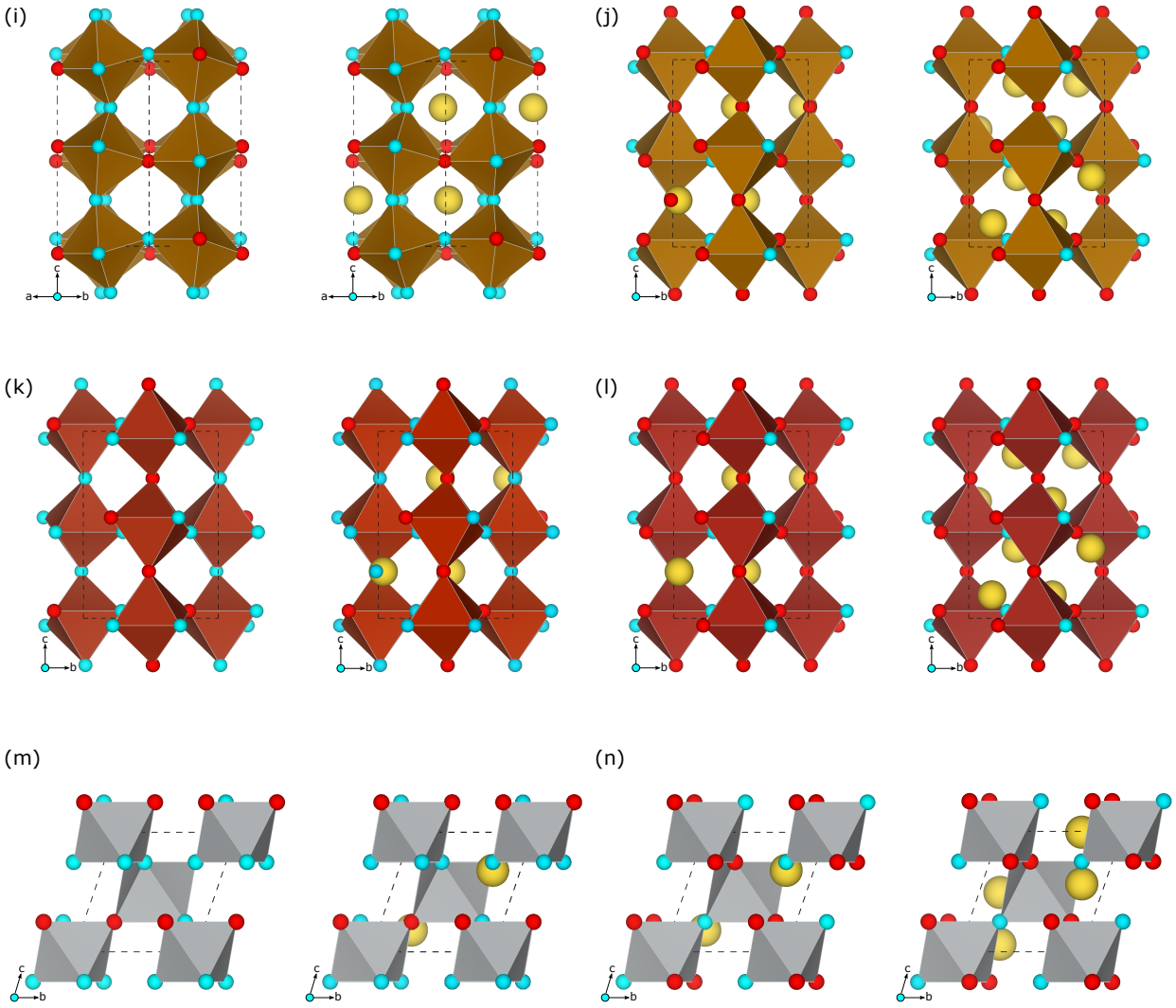

Figure S2: Initial structures of the desodiated ground states and their corresponding sodiated structures, (a) $TiOF_2$ (left) and $NaTiOF_2$ (right), (b) $NaTiO_2F$ (left) and Na_2TiO_2F (right), (c) VOF_2 and $NaVOF_2$, (d) $NaVO_2F$ and Na_2VO_2F, (e) $CrOF_2$ and $NaCrOF_2$, (f) $NaCrO_2F$ and Na_2CrO_2F, (g) $MnOF_2$ and $NaMnOF_2$, (h) $NaMnO_2F$ and Na_2MnO_2F, (i) $FeOF_2$ and $NaFeOF_2$, (i) $NaFeO_2F$ and Na_2FeO_2F, (k) $CoOF_2$ and $NaCoOF_2$, (l) $NaCoO_2F$ and Na_2CoO_2F, (m) $NiOF_2$ and $NaNiOF_2$, and (n) $NaNiO_2F$ and Na_2NiO_2F. Yellow, red, and blue spheres are Na, O, and F, respectively. Polyhedra in each panels represent the corresponding transition metal.

Literature stability data

Table S5: Comparison of thermodynamic stability data in calculated Na-M-O-F phase diagrams in this work with the Materials Project database[6] and thermochemical handbooks.[7,8] ICSD structures that do not have an equivalent entry within the Materials Project are indicated as Not available under the 'Collection ID' column under Materials Project.

ICSD COLLECTION ID	COMPOSITIONS ON PHASE DIAGRAM		COMPOSITIONS ON MATERIALS PROJECT		BOOKS ON THERMOCHEMICAL DATA
	STABLE: BLACK UNSTABLE: RED	E^{hull} (meV/atom)	COLLECTION ID	E^{hull} (meV/atom)	DATA AVAILABLE: Y DATA UNAVAILABLE: N
Na, O, F elements					
44757	Na	0	mp-127	20	Y
18311	O_2	0	mp-611836	0	Y
16262	F_2	0	mp-561203	0	Y
Na-O systems					
26583	NaO_2	0	mp-1901	0	Y
85587	NaO_3	16	mp-22464	84	N
60435	Na_2O	0	mp-2352	0	Y
26575	Na_2O_2	0	mp-2340	0	Y
Na-F systems					
29128	NaF	0	mp-682	0	Y
Ti element					
43416	Ti	0	mp-72	0	Y
Ti-O systems					
174033	$TiO_{1.25}$	49	mp-10734	56	N
15327	TiO	24	mp-1203	53	Y
9191	TiO_2	0	mp-2657	10	Y
23574	Ti_2O	0	mp-1215	0	N
6095	Ti_2O_3	0	mp-458	0	Y
20041	Ti_3O	0	mp-2591	0	N
75194	Ti_3O_5	31	mp-1147	8	Y
77697	Ti_4O_5	77	mp-10734	56	N
6098	Ti_4O_7	0	mp-12205	0	N
9038	Ti_5O_9	10	mp-748	0	N
17009	Ti_6O	0	mp-554098	0	N
35121	Ti_6O_{11}	4	mp-30524	0	N

Continued on next page

ICSD COLLECTION ID	COMPOSITIONS ON PHASE DIAGRAM		COMPOSITIONS ON MATERIALS PROJECT		BOOKS ON THERMOCHEMICAL DATA
	STABLE: BLACK UNSTABLE: RED	E^{hull} (meV/atom)	COLLECTION ID	E^{hull} (meV/atom)	DATA AVAILABLE: Y DATA UNAVAILABLE: N
Ti-O systems					
35122	Ti_7O_{13}	4	mp-556724	1	N
35123	Ti_8O_{15}	6	mp-565700	2	N
35124	Ti_9O_{17}	5	mp-27273	2	N
Ti-F systems					
65410	TiF_2	0	mp-282	248	N
16649	TiF_3	0	mp-562468	2	N
78737	TiF_4	0	mp-28974	0	Y
Na-Ti-O systems					
202906	$NaTi_2O_4$	0	mp-29356	0	N
69110	$NaTi_8O_{13}$	40	mp-28649	5	N
187821	$Na_2Ti_3O_7$	30	mp-3488	0	Y
23877	$Na_2Ti_6O_{13}$	27	mp-5446	0	N
238299	$Na_3Ti_6O_{13}$	49	mp-1190392	20	N
170677	$Na_4Ti_5O_{12}$	0	Not available		N
251700	$Na_8Ti_5O_{14}$	0	mp-28017	0	N
Na-Ti-F systems					
389	$NaTiF_4$	0	mp-27264	0	N
40916	Na_2TiF_6	0	mp-556024	0	N
Ti-O-F systems					
160661	$TiOF_2$	0	Not available		Y
Na-Ti-O-F systems					
No Na-Ti-O-F composition available					
V element					
43420	V	0	mp-146	0	Y
V-O systems					
28681	VO	0	mp-19184	22	Y
15889	VO_2	4	mp-1102963	43	Y
6286	V_2O_3	0	mp-715514	11	Y
24042	V_2O_5	0	mp-25279	0	Y
16445	V_3O_5	0	mp-622497	12	Y

Continued on next page

ICSD COLLECTION ID	COMPOSITIONS ON PHASE DIAGRAM		COMPOSITIONS ON MATERIALS PROJECT		BOOKS ON THERMOCHEMICAL DATA
	STABLE: BLACK UNSTABLE: RED	E^{hull} (meV/atom)	COLLECTION ID	E^{hull} (meV/atom)	DATA AVAILABLE: Y DATA UNAVAILABLE: N
V-O systems					
2338	V_3O_7	0	mp-622640	20	N
2775	V_4O_7	4	mp-555597	37	Y
15041	V_4O_9	17	mp-27412	45	N
6097	V_5O_9	0	mp-542334	30	N
196	V_6O_{11}	3	mp-30518	39	N
15028	V_6O_{13}	0	mp-18896	45	Y
77706	V_7O_3	77	mp-542910	831	N
197	V_7O_{13}	0	mp-27151	45	N
166600	V_8O	46	mp-714972	1378	N
424885	V_8O_{15}	3	mp-556566	42	N
424886	V_9O_{17}	2	mp-559485	57	N
77708	$V_{13}O_{16}$	204	mp-30065	677	N
77707	$V_{16}O_3$	31	mp-30064	1396	N
V-F systems					
32552	VF_2	0	mp-555934	0	N
30624	VF_3	0	mp-559931	0	Y
65785	VF_4	0	Not available		Y
9887	VF_5	0	mp-27309	0	Y
Na-V-O systems					
420136	$NaVO_2$	0	mp-19391	0	N
29450	$NaVO_3$	53	mp-555665	6	Y
159905	NaV_2O_4	57	mp-642750	21	N
92955	NaV_2O_5	0	Not available		N
71869	NaV_6O_{11}	105	mp-555198	396	N
32262	NaV_3O_8	110	Not available		N
239394	$Na_{0.33}V_2O_5$	83	Not available		N
20556	$Na_2(VO_3)_2$	54	mp-19083	0	N
163234	$Na_2V_3O_7$	138	mp-557315	0	N
35635	$Na_4V_2O_7$	0	mp-648893	5	Y
280067	$Na_{4.5}V_7O_{17.5}$	171	Not available		N

Continued on next page

ICSD COLLECTION ID	COMPOSITIONS ON PHASE DIAGRAM		COMPOSITIONS ON MATERIALS PROJECT		BOOKS ON THERMOCHEMICAL DATA
	STABLE: BLACK UNSTABLE: RED	E^{hull} (meV/atom)	COLLECTION ID	E^{hull} (meV/atom)	DATA AVAILABLE: Y DATA UNAVAILABLE: N
Na-V-O systems					
416170	Na_5VO_4O	0	mp-18233	2	N
55686	$Na_{1.286}V_2O_5$	167	Not available		N
194368	$Na_{0.5}VO_2$	97	mp-783905	17	N
Na-V-F systems					
60611	$NaVF_3$	0	mp-20572	91	N
407013	$NaVF_4$	0	mp-17999	0	Y
27347	Na_3VF_6	0	mp-556633	37	Y
V-O-F systems					
142594	VOF_2	0	Not available		N
249507	VOF_3	0	mp-556026	0	N
Na-V-O-F systems					
No Na-V-O-F composition available					
Cr element					
44731	Cr	0	mp-90	0	Y
Cr-O systems					
109296	CrO	337	mp-19091	368	Y
9423	CrO_2	0	mp-19177	0	Y
16031	CrO_3	46	mp-510421	47	Y
25781	Cr_2O_3	0	mp-19399	0	Y
15904	Cr_3O	1612	mp-20609	1808	N
24299	Cr_5O_{12}	0	mp-13869	25	N
71297	Cr_8O_{21}	18	mp-558855	33	N
Cr-F systems					
31827	CrF_2	82	mp-554340	0	Y
25828	CrF_3	0	mp-560338	0	Y
78778	CrF_4	0	mp-20488	6	Y
419661	CrF_5	0	mp-639662	0	N
14135	Cr_2F_5	41	mp-558380	3	N
Na-Cr-O systems					
182235	$NaCrO_2$	0	mp-578604	0	Y

Continued on next page

ICSD COLLECTION ID	COMPOSITIONS ON PHASE DIAGRAM		COMPOSITIONS ON MATERIALS PROJECT		BOOKS ON THERMOCHEMICAL DATA
	STABLE: BLACK UNSTABLE: RED	E^{hull} (meV/atom)	COLLECTION ID	E^{hull} (meV/atom)	DATA AVAILABLE: Y DATA UNAVAILABLE: N
Na-Cr-O systems					
82620	$NaCr(CrO_4)_2$	0	mp-19280	0	N
235826	$NaCr_2O_4$	1	Not available		N
159511	Na_2CrO_4	0	mp-18779	0	Y
2771	$Na_2Cr_2O_7$	0	mp-704459	0	Y
62676	Na_4CrO_4	0	mp-18884	0	N
Na-Cr-F systems					
25428	$NaCrF_3$	75	Not available		N
37108	$NaCrF_4$	0	mp-17523	0	N
418670	$NaCrF_6$	0	mp-646192	0	N
67250	Na_2CrF_4	98	mp-558383	12	N
27070	Na_3CrF_6	8	mp-560929	0	N
150870	$Na_5Cr_3F_{14}$	0	mp-561252	7	N
Cr-O-F systems					
59123	$CrOF_3$	144	mp-31703	193	N
249513	CrO_2F_2	154	mp-606313	188	N
Na-Cr-O-F systems					
No Na-Cr-O-F composition available					
Mn element					
5248	Mn	0	mp-1055908	370	Y
Mn-O systems					
9864	MnO	0	mp-19006	53	Y
393	MnO_2	0	mp-510408	6	Y
24342	Mn_2O_3	0	mp-1172875	0	Y
60821	Mn_2O_7	719	mp-28338	336	N
8355	Mn_3O_4	0	mp-18759	0	Y
16956	Mn_5O_8	2	mp-18922	13	N
Mn-F systems					
14142	MnF_2	0	mp-560902	0	Y
19080	MnF_3	0	mp-556560	0	N
62068	MnF_4	0	mp-541103	0	N

Continued on next page

ICSD COLLECTION ID	COMPOSITIONS ON PHASE DIAGRAM		COMPOSITIONS ON MATERIALS PROJECT		BOOKS ON THERMOCHEMICAL DATA
	STABLE: BLACK UNSTABLE: RED	E^{hull} (meV/atom)	COLLECTION ID	E^{hull} (meV/atom)	DATA AVAILABLE: Y DATA UNAVAILABLE: N
Mn-F systems					
113572	Mn_2F_5	0	mp-753169	74	N
113573	Mn_3F_8	12	Not available		N
Na-Mn-O systems					
151587	$NaMn_3Mn_4O_{12}$	13	mp-18999	29	N
431105	$NaMnO_4$	322	mp-765753	69	Y
16270	$NaMnO_2$	0	mp-18957	0	N
172604	$NaMn_2O_4$	0	mp-542710	0	N
19022	$NaMn_7O_{12}$	16	mp-18999	0	N
1563	$Na_{14}(MnO_4)_2O$	0	mp-27569	0	N
419587	Na_2MnO_2	0	mp-559081	6	N
39504	Na_2MnO_4	107	mp-28186	84	Y
409981	$Na_2Mn_2O_3$	9	mp-558376	0	N
92858	$Na_2Mn_3O_7$	0	mp-61050	0	N
1026	$Na_4Mn_2O_5$	0	mp-1026	0	N
47101	Na_5MnO_4	19	mp-28262	10	N
420410	Na_6MnO_4	16	mp-19321	18	N
Na-Mn-F systems					
15621	$NaMnF_3$	0	mp-560242	0	N
15621	$NaMnF_4$	0	mp-554517	0	N
62080	$NaMn_3F_{10}$	8	mp-541104	0	N
62080	Na_2MnF_5	0	mp-555618	0	N
66315	Na_3MnF_6	0	mp-561200	159	N
62788	$Na_5Mn_3F_{14}$	9	mp-28398	14	N
Mn-O-F systems					
No Mn-O-F composition available					
Na-Mn-O-F systems					
No Na-Mn-O-F composition available					
Fe element					
14754	Fe	0	mp-13	0	Y
Fe-O systems					

Continued on next page

ICSD COLLECTION ID	COMPOSITIONS ON PHASE DIAGRAM		COMPOSITIONS ON MATERIALS PROJECT		BOOKS ON THERMOCHEMICAL DATA
	STABLE: BLACK UNSTABLE: RED	E^{hull} (meV/atom)	COLLECTION ID	E^{hull} (meV/atom)	DATA AVAILABLE: Y DATA UNAVAILABLE: N
Fe-O systems					
31081	FeO	0	mp-18905	410	Y
7797	Fe_2O_3	0	mp-19770	0	Y
5247	Fe_3O_4	0	mp-19306	0	Y
434152	Fe_4O_5	87	Not available		N
430563	Fe_5O_7	143	mp-1095382	171	N
430601	Fe_7O_9	100	Not available		N
135154	Fe_7O_{10}	152	Not available		N
238770	$Fe_{13}O_{19}$	277	mp-1195927	303	N
430562	$Fe_{25}O_{32}$	188	Not available		N
Fe-F systems					
9166	FeF_2	0	mp-556911	0	Y
41120	FeF_3	0	mp-22398	0	Y
Na-Fe-O systems					
37157	$NaFeO_2$	0	mp-19359	0	Y
200009	$NaFe_2O_3$	65	mp-18728	101	N
1118	$Na_{14}Fe_6O_{16}$	24	mp-18917	22	N
50478	Na_2FeO_4	170	mp-19044	71	N
413270	Na_3FeO_3	6	mp-30947	0	N
14353	$Na_3Fe_5O_9$	88	mp-540658	8	N
1410	Na_4FeO_3	0	mp-19026	15	N
59585	Na_4FeO_4	0	mp-19022	0	N
73881	$Na_4Fe_{12}O_{20}$	54	mp-505170	71	N
1025	$Na_4Fe_2O_5$	48	mp-19396	38	N
2485	Na_5FeO_4	1	mp-13745	5	N
1557	$Na_8Fe_2O_7$	0	mp-27557	0	N
412212	$Na_9FeO_3FeO_4$	3	mp-16398	22	N
Na-Fe-F systems					
32384	$NaFeF_3$	0	mp-505066	0	Y
15501	$NaFeF_4$	0	mp-18455	0	N
67957	$Na_2Fe_2F_7$	7	mp-1203434	16	N

Continued on next page

ICSD COLLECTION ID	COMPOSITIONS ON PHASE DIAGRAM		COMPOSITIONS ON MATERIALS PROJECT		BOOKS ON THERMOCHEMICAL DATA
	STABLE: BLACK UNSTABLE: RED	E^{hull} (meV/atom)	COLLECTION ID	E^{hull} (meV/atom)	DATA AVAILABLE: Y DATA UNAVAILABLE: N
Na-Fe-F systems					
20157	Na_3FeF_6	0	mp-560311	0	N
150871	$Na_5Fe_3F_{14}$	10	mp-560925	2	N
Fe-O-F systems					
No Fe-O-F composition available					
Na-Fe-O-F systems					
No Na-Fe-O-F composition available					
Co element					
36675	Co	0	mp-54	30	Y
Co-O systems					
9865	CoO	25	mp-19079	37	Y
88722	CoO_2	377	mp-32686	107	N
24210	Co_3O_4	0	mp-18748	10	Y
Co-F systems					
9167	CoF_2	0	mp-555908	0	Y
16672	CoF_3	0	mp-559473	52	Y
Na-Co-O systems					
6152	$NaCoO_2$	0	mp-18921	0	N
155491	$Na_{0.5}CoO_2$	0	mp-22474	0	N
162855	$Na_{0.571}CoO_2$	49	Not available		N
167343	$Na_{0.667}CoO_2$	59	mp-1203207	55	N
413025	$Na_{10}Co_4O_{10}$	20	mp-561875	6	N
10064	$Na_{10}Co_4O_9$	0	mp-562435	0	N
73211	Na_3CoO_2	3	mp-28824	30	N
10473	Na_4CoO_3	0	mp-18762	0	N
4196	Na_4CoO_4	0	mp-760068	0	N
14180	Na_5CoO_4	6	mp-21792	0	N
99580	$Na_6Co_2O_6$	9	mp-31126	0	N
414127	$Na_7(CoO_3)_2$	11	mp-19427	12	N
99917	$Na_9Co_2O_7$	12	mp-510308	14	N
Na-Co-F systems					

Continued on next page

ICSD COLLECTION ID	COMPOSITIONS ON PHASE DIAGRAM		COMPOSITIONS ON MATERIALS PROJECT		BOOKS ON THERMOCHEMICAL DATA
	STABLE: BLACK UNSTABLE: RED	E^{hull} (meV/atom)	COLLECTION ID	E^{hull} (meV/atom)	DATA AVAILABLE: Y DATA UNAVAILABLE: N
Na-Co-F systems					
4404	$NaCoF_3$	0	mp-521404	0	N
Co-O-F systems					
No Co-O-F composition available					
Na-Co-O-F systems					
No Na-Co-O-F composition available					
Ni element					
8688	Ni	0	mp-23	0	Y
Ni-O systems					
9866	NiO	0	mp-19009	0	Y
78698	NiO_2	150	mp-25210	131	N
Ni-F systems					
9168	NiF_2	0	mp-559798	0	Y
87944	NiF_3	0	mp-614777	0	N
Na-Ni-O systems					
85317	$NaNiO_2$	351	mp-21792	0	N
14159	Na_2NiO_2	0	mp-18765	43	N
1583	Na_5NiO_4	421	mp-21996	0	N
Na-Ni-F systems					
25533	$NaNiF_3$	0	mp-561480	0	N
26073	Na_3NiF_6	0	mp-554649	0	N
138821	$NiNa_2F_6$	0	Not available		N
Ni-O-F systems					
No Ni-O-F composition available					
Na-Ni-O-F systems					
No Na-Ni-O-F composition available					

Extent of Jahn-Teller distortion

Table S6: Percentage deviation in lattice parameters (b/a and c/a) upon DFT energy calculation as a result of Jahn Teller distortion observed in sodiated F and O-rich Ni and Mn oxyfluorides, respectively.

$NaMnOF_2$			Na_2MnO_2F		
b/a INITIAL	**b/a RELAXED**	**% DEVIATION**	**b/a INITIAL**	**b/a RELAXED**	**% DEVIATION**
1	1	0.20	1.01	1.33	31.52
c/a INITIAL	**c/a RELAXED**	**% DEVIATION**	**c/a INITIAL**	**c/a RELAXED**	**% DEVIATION**
1.03	0.97	-5.36	1.40	1.24	-11.02

$NaNiOF_2$			Na_2NiO_2F		
b/a INITIAL	**b/a RELAXED**	**% DEVIATION**	**b/a INITIAL**	**b/a RELAXED**	**% DEVIATION**
1	0.99	-1.33	1	1.08	7.53
c/a INITIAL	**c/a RELAXED**	**% DEVIATION**	**c/a INITIAL**	**c/a RELAXED**	**% DEVIATION**
1.03	0.98	-4.13	1.03	1.25	21.46

Tolerance Factors

Table S7: Calculated Goldschmidt (t)[9] and Bartel et al. (τ)[10] tolerance factors for $AMOF_2$, AMO_2F, and A_2MO_2F (A = Na or Li). Values outside the tolerance factor thresholds for forming a perovskite structure, namely $0.825 < t < 1.059$ and $\tau < 4.18$, are highlighted with red text.

M	$AMOF_2$				AMO_2F				A_2MO_2F			
	A= Na		A= Li		A= Na		A= Li		A= Na		A= Li	
	t	τ	t	τ	t	τ	t	τ	t	τ	t	τ
Ti	0.959	3.863	0.794	5.350	0.956	3.898	0.793	5.385	0.956	3.898	0.793	5.385
V	0.973	3.915	0.806	5.076	0.970	3.951	0.805	5.112	0.970	3.951	0.805	5.112
Cr	0.986	3.972	0.817	4.915	1.015	4.229	0.843	4.754	0.982	4.010	0.815	4.953
Mn	0.971	3.905	0.804	5.115	1.026	4.318	0.852	4.745	0.968	3.941	0.803	5.151
Fe	0.971	3.905	0.804	5.115	0.997	4.099	0.828	4.827	0.968	3.941	0.803	5.151
Co	0.988	3.985	0.819	4.889	1.026	4.318	0.852	4.745	0.985	4.024	0.817	4.927
Ni	0.993	4.013	0.823	4.843	1.054	4.592	0.875	4.814	0.990	4.052	0.822	4.882
Mo	0.949	3.838	0.787	5.596	0.965	3.931	0.801	5.192	0.947	3.872	0.786	5.630
Nb	0.936	3.814	0.775	6.092	0.951	3.884	0.790	5.500	0.933	3.847	0.775	6.125

Decomposition products

Table S8: Predicted decomposition products of metastable/unstable O-rich and F-rich perovskites considered in this work.

TRANSITION METAL	OXYFLUORIDE COMPOSITION	PREDICTED DECOMPOSITION PRODUCTS
Ti	$NaTiOF_2$	Ti_2O_3, $NaTiF_4$, NaF
	$NaTiO_2F$	TiO_2, NaF
	Na_2TiO_2F	Ti_2O_3, $Na_8Ti_5O_{14}$, NaF, Na
V	$NaVOF_2$	V_2O_3, Na_3VF_6
	$NaVO_2F$	V_2O_3, Na_3VF_6, NaV_2O_5, NaF
	Na_2VO_2F	$NaVO_2$, NaF
Cr	$CrOF_2$	Cr_5O_{12}, CrF_3, O_2
	$NaCrOF_2$	Na_3CrF_6, Cr_2O_3
	$NaCrO_2F$	CrO_2, NaF
	Na_2CrO_2F	$NaCrO_2$, NaF
Mn	$MnOF_2$	MnO_2, MnF_3, O_2
	$NaMnOF_2$	Mn_2O_3, Na_3MnF_6
	$NaMnO_2F$	MnO_2, NaF
	Na_2MnO_2F	$NaMnO_2$, NaF
Fe	$FeOF_2$	Fe_2O_3, FeF_3, O_2
	$NaFeOF_2$	Na_3FeF_6, Fe_2O_3
	$NaFeO_2F$	Fe_2O_3, O_2, NaF
	Na_2FeO_2F	$NaFeO_2$, NaF
Co	$CoOF_2$	CoF_2, O_2
	$NaCoOF_2$	$Na_{0.5}CoO_2$, $NaCoF_3$, O_2, NaF
	$NaCoO_2F$	$Na_{0.5}CoO_2$, $NaCoF_3$, O_2, NaF
	Na_2CoO_2F	$NaCoO_2$, NaF
Ni	$NiOF_2$	NiF_2, O_2
	$NaNiOF_2$	$NaNiF_3$, Na_2NiO_2, NiF_2, O_2
	$NaNiO_2F$	Na_2NiO_2, NiF_2, O_2
	Na_2NiO_2F	$NaNiF_3$, Na_2NiO_2, O_2, NaF

Intercalation vs. conversion voltages

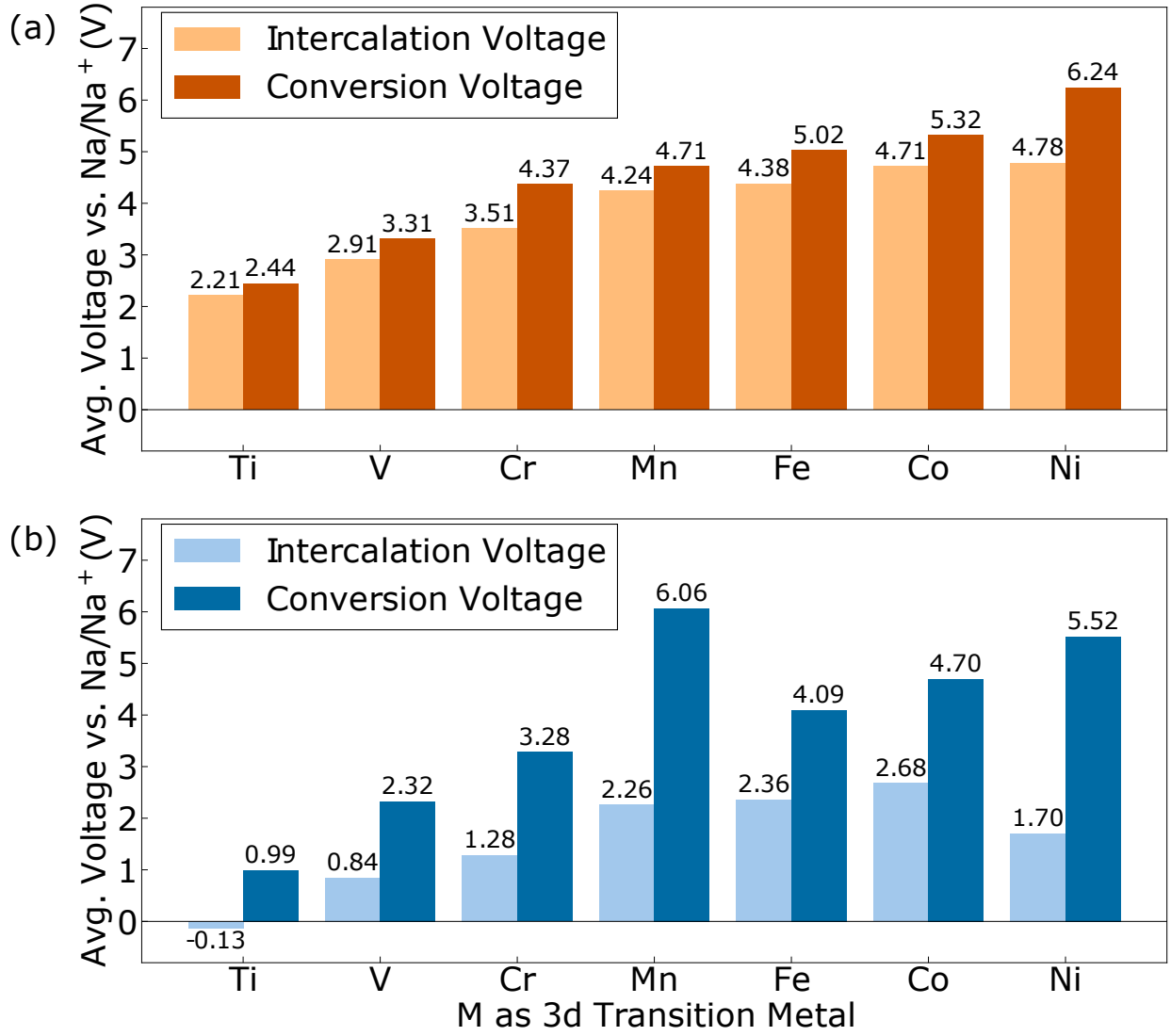

Figure S3: Comparison of intercalation (light colored bars) and conversion (dark colored bars) voltages for (a) $MOF_2 \leftrightarrow NaMOF_2$, and (b) $NaMO_2F \leftrightarrow Na_2MO_2F$ systems. Typically, larger conversion voltages compared to intercalation voltages indicate larger thermodynamic driving force for cathode materials to decompose into thermodynamically stable product(s) (see Table **S8**). rather than undergoing intercalation.

0 K phase diagrams

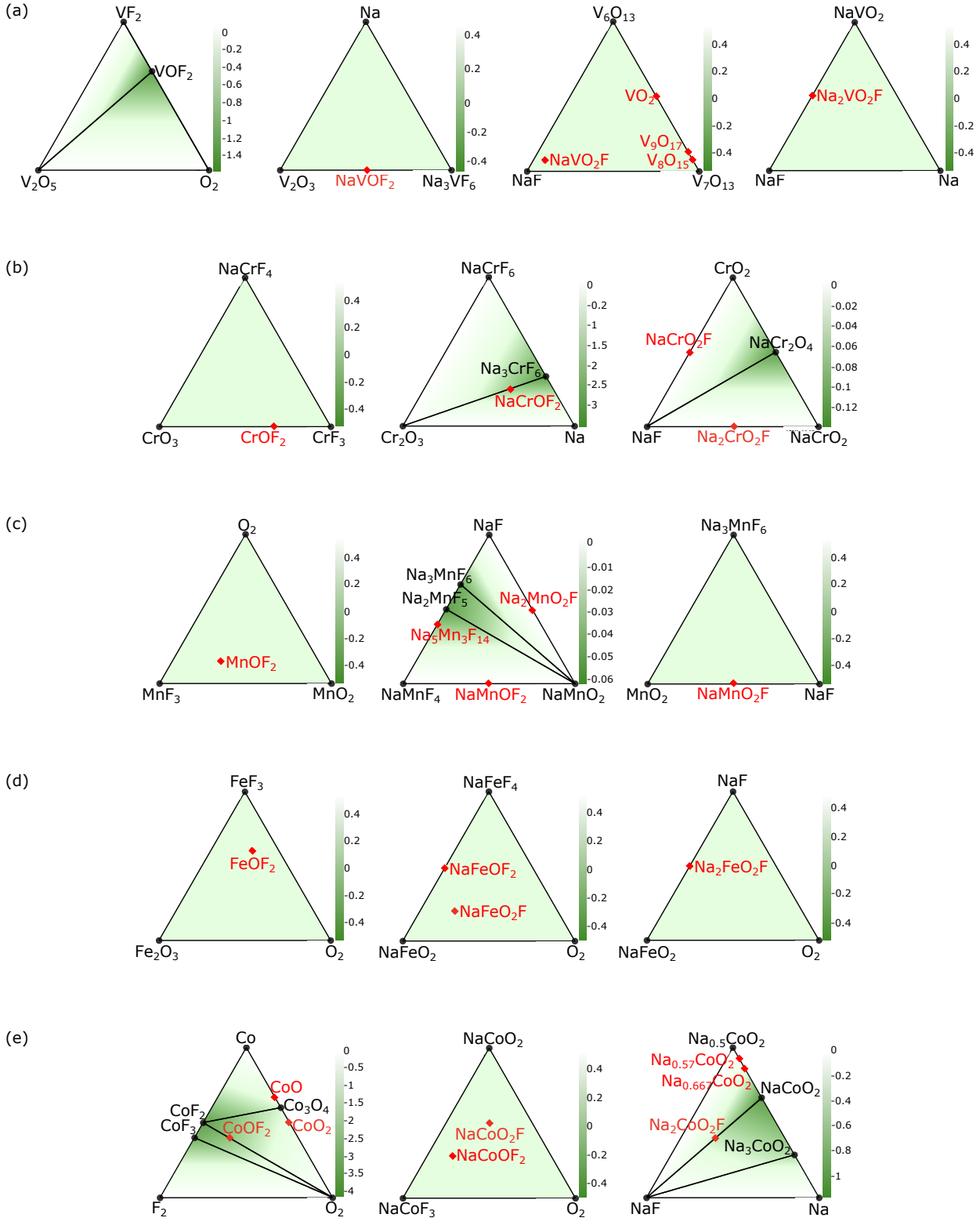

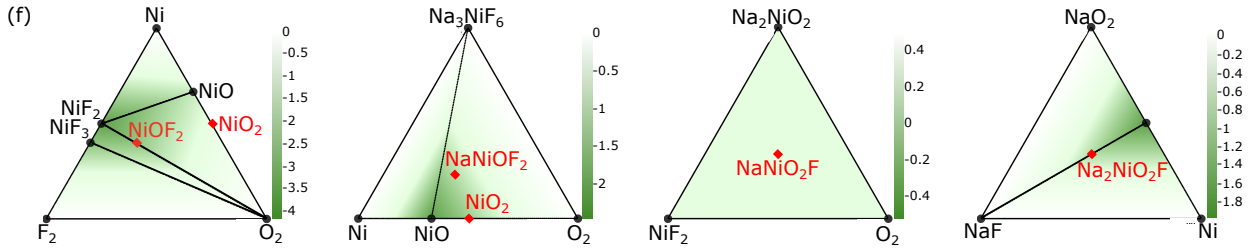

Figure S4: Ternary projections of quaternary phase diagrams of (a) Na-V-O-F, (b) Na-Cr-O-F, (c) Na-Mn-O-F, (d) Na-Fe-O-F, (e) Na-Co-O-F, and, (f) Na-Ni-O-F. Annotations used in this figure are identical to **Figure 5** of the main text.

Minimum energy pathways (MEPs)

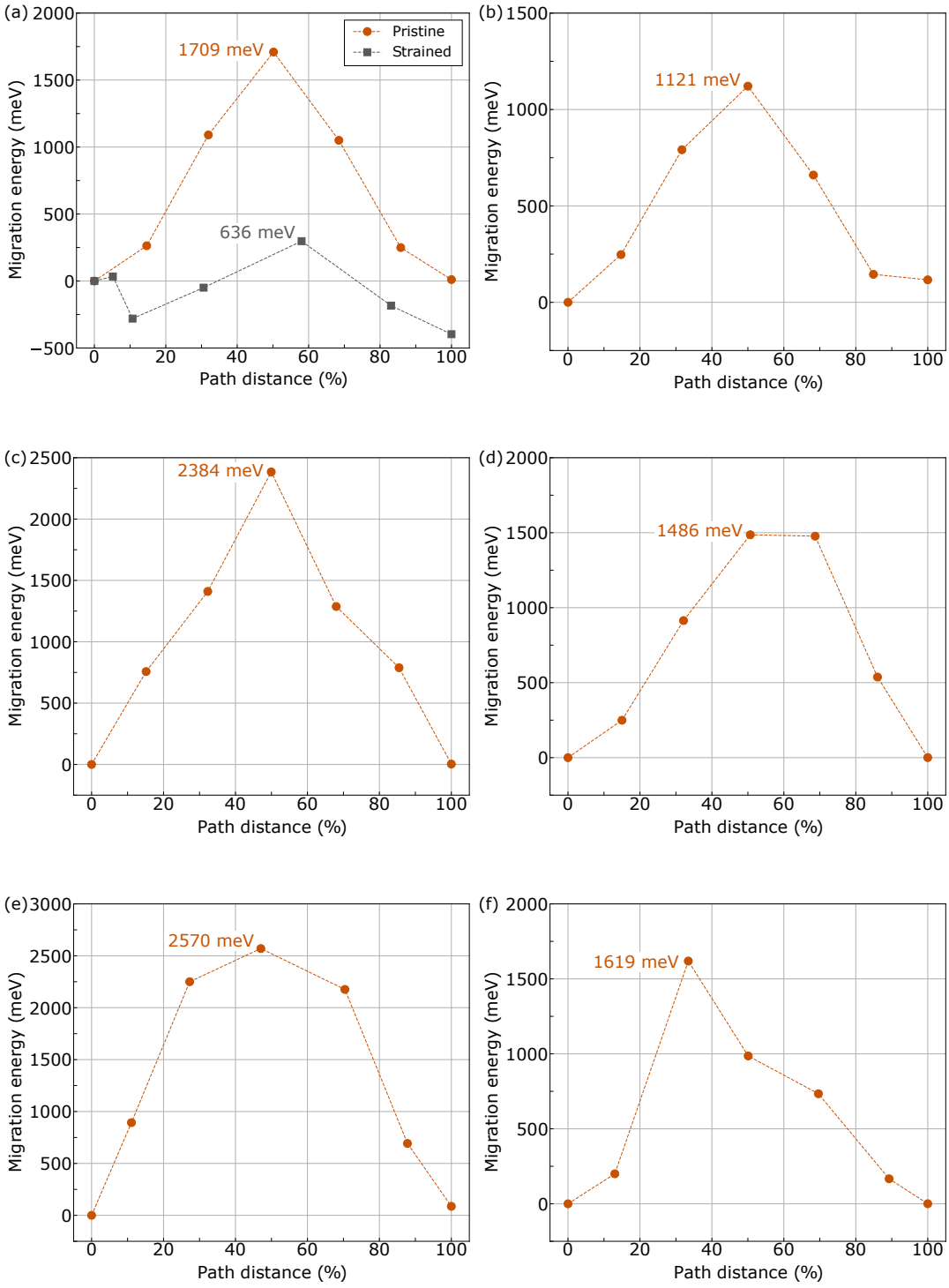

Figure S5: Calculated Na^+ MEPs for the candidate perovskite oxyfluorides, namely, (a) $TiOF_2$, (b) $NaTiOF_2$, (c) VOF_2, (d) $NaVOF_2$, (e) $CrOF_2$, and (d) $NaMnOF_2$. The E_m values are listed as text annotations in each panel. In panel (a), the MEP for the homogeneously strained $TiOF_2$ structure is shown with grey squares and the E_m in grey text.

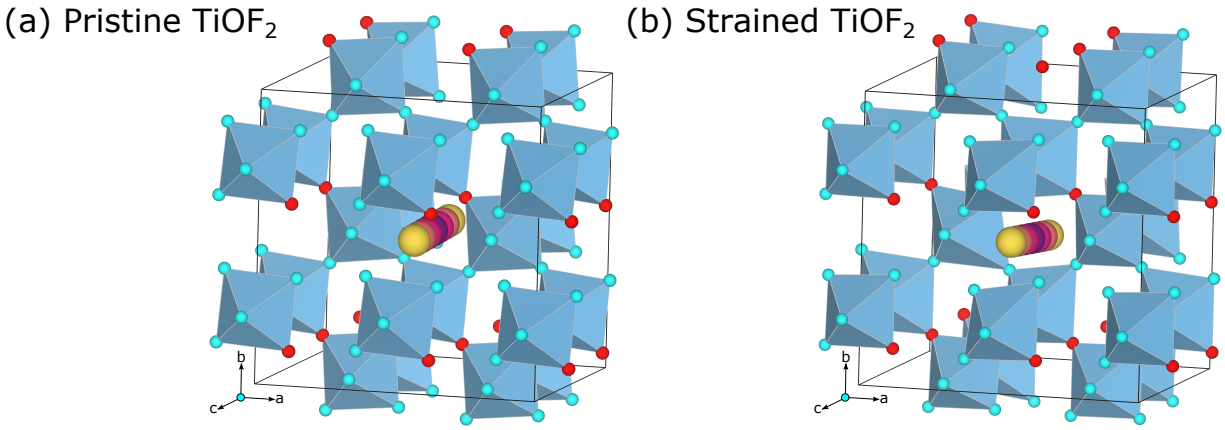

Figure S6: Na^+ mobility pathway shown for a candidate perovskite oxyfluoride, namely, (a) pristine $TiOF_2$, and (b) 5% homogeneously strained $TiOF_2$. The yellow, orange, pink and purple balls along the mobility pathway represent the images of migrating Na^+ from one site (yellow) to another vacant (yellow) site. The average Na-O/F bond-distances at the transition state image were initialized at (relaxed to) 1.90 Å (1.91 Å) and 2.05 Å (2.41 Å) in pristine and strained $TiOF_2$, respectively.

References

(1) Reddy, M.; Madhavi, S.; Rao, G. S.; Chowdari, B. Metal oxyfluorides $TiOF_2$ and NbO_2F as anodes for Li-ion batteries. *Journal of power sources* **2006**, *162*, 1312–1321.

(2) Kuhn, A.; Plews, M. R.; Pérez-Flores, J. C.; Fauth, F.; Hoelzel, M.; Cabana, J.; García-Alvarado, F. Redox Chemistry and Reversible Structural Changes in Rhombohedral VO_2F Cathode during Li Intercalation. *Inorganic chemistry* **2020**, *59*, 10048–10058.

(3) Long, O. Y.; Gautam, G. S.; Carter, E. A. Evaluating optimal U for 3 d transition-metal oxides within the SCAN+ U framework. *Physical Review Materials* **2020**, *4*, 045401.

(4) Tekliye, D. B.; Gautam, G. S. Accuracy of metaGGA functionals in describing transition metal fluorides. *arXiv preprint arXiv:2401.10832* **2024**,

(5) Hellenbrandt, M. The inorganic crystal structure database (ICSD)—present and future. *Crystallography Reviews* **2004**, *10*, 17–22.

(6) Jain, A.; Ong, S. P.; Hautier, G.; Chen, W.; Richards, W. D.; Dacek, S.; Cholia, S.; Gunter, D.; Skinner, D.; Ceder, G.; others Commentary: The Materials Project: A materials genome approach to accelerating materials innovation. *APL materials* **2013**, *1*.

(7) Kubaschewski, O.; Alcock, C. B.; Spencer, P. Materials thermochemistry. *(No Title)* **1993**,

(8) Wagman, D. D.; Evans, W. H.; Parker, V. B.; Schumm, R. H.; Halow, I.; Bailey, S. M.; Churney, K. L.; Nuttall, R. L. Erratum: The NBS tables of chemical thermodynamic properties. Selected values for inorganic and C1 and C2 organic substances in SI units [J. Phys. Chem. Ref. Data 11, Suppl. 2 (1982)]. *Journal of Physical and Chemical Reference Data* **1989**, *18*, 1807–1812.

(9) Goldschmidt, V. M. Die gesetze der krystallochemie. *Naturwissenschaften* **1926**, *14*, 477–485.

(10) Bartel, C. J.; Sutton, C.; Goldsmith, B. R.; Ouyang, R.; Musgrave, C. B.; Ghiringhelli, L. M.; Scheffler, M. New tolerance factor to predict the stability of perovskite oxides and halides. *Science advances* **2019**, *5*, eaav0693.